

This manuscript is titled **A New Fault Model for the 1933 Long Beach Earthquake, Long Beach Area, Southern California**. The authors are Dan Gish (dgish@3dseismicsolutions.com) and Steve Boljen (sboljen@3dseismicsolutions.com). This manuscript has been submitted for review to *Seismica*.

The manuscript is undergoing peer review and has yet to be formally accepted for publication. Subsequent versions of this manuscript may have slightly different content.

If accepted, the final version of this manuscript will be available via the 'Peer-reviewed Publication DOI' link on the right-hand side of this webpage.

Please feel free to contact any of the authors; we welcome feedback.

1 **A New Fault Model for the 1933 Long Beach Earthquake,**
2 **Long Beach Area, Southern California**

3 Dan Gish¹, Steve Boljen²

4 ¹ 3D Seismic Solutions, 811 Birchwood Circle, Council Bluffs, IA 51503

5 ² 3D Seismic Solutions, 316 Silver Creek Landing Road, Peletier, NC 28584

6 Corresponding Author: sboljen@3dseismicsolutions.com

7

8 **Abstract**

9 Newly identified thrust faults and their corresponding thrust sheets, combined with recent
10 micro-earthquake epicenters, better explain anomalous rupture data observed during the
11 1933 Long Beach Earthquake than previous models based exclusively on Newport-
12 Inglewood Fault Zone strike-slip faulting. A high-quality 45 km² 3D seismic dataset was
13 recorded in 2017, centered along the Seal Beach Anticline, providing direct confirmation of
14 a much more complex system of previously unrecognized thrust faults and cross faults
15 encompassing the east flank of Wilmington Anticline, Seal Beach Anticline, and Los
16 Alamitos Anticline, extending onshore at least 6 miles into the Los Angeles Basin.
17 Additionally, more than 1200 micro-earthquakes recorded by a dense seismic network
18 during 2017 have been located several miles to either side of the NIFZ and correlate with
19 the newly identified thrust sheets and areas of recent deformation, indicating the faults are
20 active. Based on this new fault model, energy propagation from the 1933 Earthquake

21 appears to have transitioned from essentially pure horizontal strike-slip displacement
22 along the NIFZ at its southern epicenter to high vertical-component transpressional
23 displacement upon encountering the Garden Grove Fault – Coastal Fault thrust salient at
24 the southern end of Seal Beach Anticline near Seal Beach Naval Weapons Station.

25

26 **Non-Technical Summary**

27 Newly identified thrust faults combined with recent micro-earthquake epicenters better
28 explain the anomalous and extreme surface damage observed during the 1933 Long Beach
29 Earthquake. Previous studies have attributed the earthquake’s damage exclusively to the
30 Newport-Inglewood Fault Zone strike-slip movement. A high-quality 45 km² 3D seismic
31 dataset that was recorded in 2017 provides confirmation of a much more complex system
32 of previously unrecognized thrust faults and cross faults encompassing the Long Beach-
33 Seal Beach area. Additionally, more than 1200 micro-earthquakes recorded by the dense
34 seismic network, located several miles to either side of the Newport-Inglewood Fault Zone,
35 have been incorporated into the database and correlate with the newly identified thrust
36 sheets and areas of recent deformation, indicating the thrust faults are active. The Alquist-
37 Priolo Act (enacted in 1972 and revised multiple times since) authorizes ongoing
38 investigations to identify potential fault zones that may reactivate and harm existing urban
39 centers. This study has identified the main faults responsible, not the Newport-Inglewood
40 Fault Zone, for the widespread destruction resulting from the 1933 Long Beach earthquake
41 and provides evidence that these newly discovered faults are currently active.

42

43 **1. Introduction**

44 The Magnitude 6.4 1933 Long Beach Earthquake, one of the most devastating
45 earthquakes to hit coastal California in recorded history, historically has presented a
46 conundrum to geoscientists, civil engineers, and legislators who have attempted to explain
47 and model the extreme earthquake parameters, design appropriate infrastructure
48 guidelines, and legislate future risk policies for expanding urban developments. The
49 epicenter for the initial 1933 event has been determined to have initiated a few miles
50 offshore from Huntington Beach as “pure dextral” strike slip displacement along a near
51 vertical plane with a dip of 80 degrees, striking northwest at 315 degrees, which
52 subsequently propagated northwest in at least two distinct sub-events along the Newport-
53 Englewood Fault Zone (NIFZ) for approximately 8-10 miles (13-16 km), before terminating
54 near Signal Hill Anticline (Haucksson and Gross, 1991; Hough and Graves, 2020).
55 Interestingly, epicenters of the aftershock sequence were determined to lie within a region
56 roughly 9-11 miles (15-18 km) wide, rather than being tightly focused along the NIFZ surface
57 location as might be expected, most of which were located east of the NIFZ.

58 Unusually extreme surface damage occurred within the Long Beach area, famously
59 evidenced by the collapse of 70 brick school buildings and damage to 50 others, ultimately
60 resulting in 120 fatalities. Shortly thereafter, legislation was passed in the form of the Field
61 Act to investigate the cause of the devastation and make recommendations to minimize
62 future occurrences. Today, the Alquist-Priolo Act (enacted in 1972 and revised multiple

63 times since) authorizes ongoing investigations to identify potential fault zones that may
64 reactivate and harm existing urban centers. One of the primary goals of these studies has
65 been to better identify and quantify the enigmatic NIFZ, assumed to be a right-lateral strike
66 slip fault zone historically associated with the 1933 Long Beach Earthquake, and believed
67 to extend for 47 miles (75.6 km) through the Los Angeles Basin (Haucksson and
68 Gross, 1991).

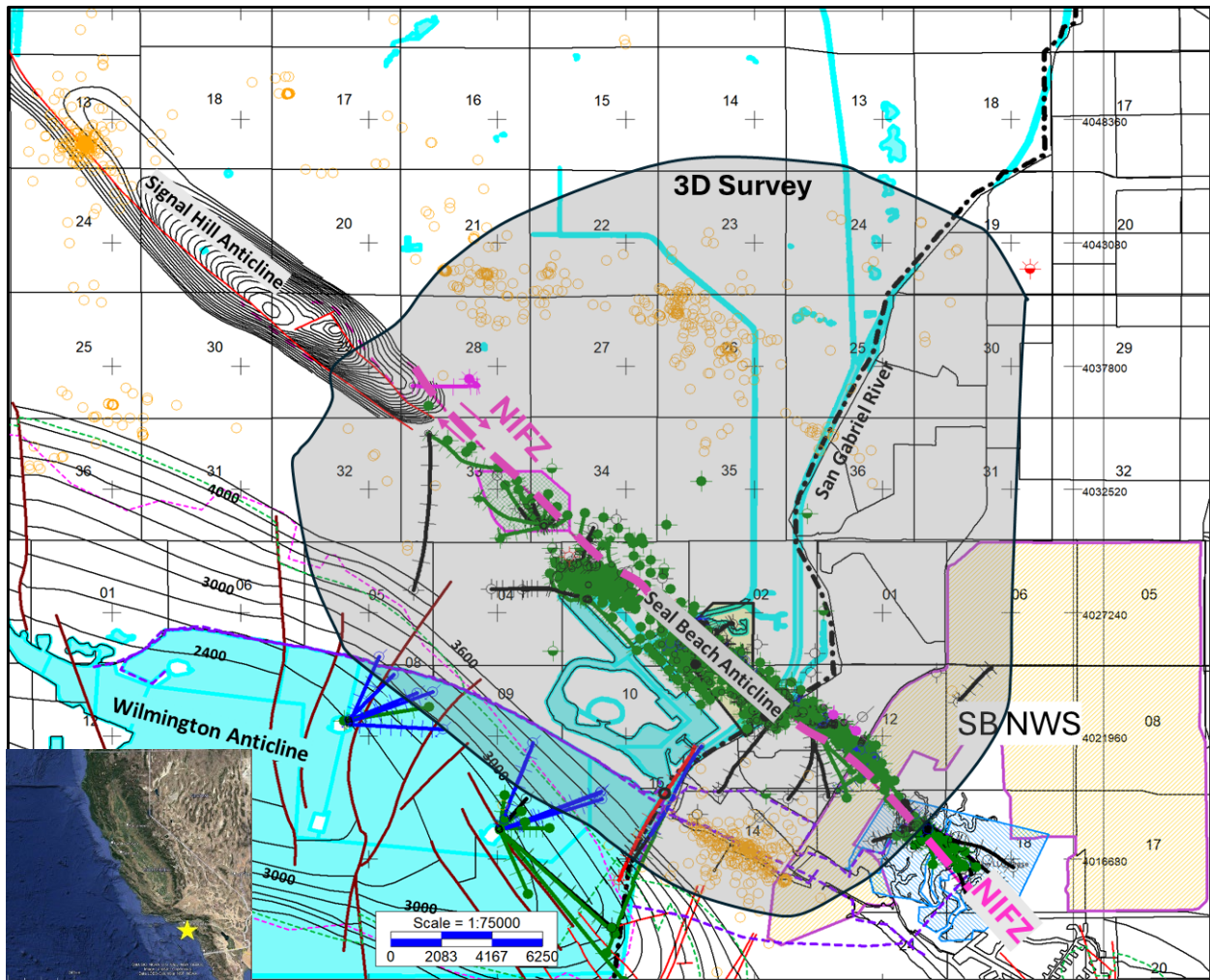
69 Primarily based on unconstrained log correlations from antique oil wells drilled along
70 the Seal Beach Anticline (SBA), numerous investigators have assigned fault plane
71 interpretations to the narrowly clustered well logs and to a few surface exposures also
72 assumed to be NIFZ faults, and have extrapolated those correlations for miles along a NW-
73 SE orientation and vertically nearly 14,000 feet from the surface into basement. When the
74 fault correlations mandate, the NIFZ has been depicted as having as many as five fault
75 splays at some locations along trend. Still today, modern fault maps of the Seal Beach
76 segment depict the NIFZ fault zone as a questionable dotted line (California Geological
77 Survey, California Department of Conservation, Seismic Hazards Program, Earthstar
78 Geographics).

79 However, significant problems arise with NIFZ-focused, strike-slip interpretations along
80 the SBA because of many conflicting observations, for example:

- 81 1. No surface rupture from the M6.4 event was observed along the SBA trend
82 corresponding to the mapped NIFZ surface trace.

- 83 2. Aftershocks following the 1933 event occurred predominantly onshore east of SBA
84 over a width of approximately 10 miles (17 km) and do not align along a linear, near-
85 vertical NIFZ trend, nor do they align with the 1933 Long Beach Earthquake
86 epicenter for the main event (Haucksson and Gross,1991).
- 87 3. During 2017, ~1200 micro-earthquake epicenters recorded by a dense
88 seismometer array (Figure 1) were detected along northwest-southeast trending
89 clusters on both flanks of the NIFZ, but not along the NIFZ itself (Yang and
90 Clayton,2021).
- 91 4. Extensive deformation of low depositional energy Pleistocene sediments are
92 apparent on 3D seismic data, on either side of SBA, miles away from the NIFZ.
93 These deformation areas correspond to previously unrecognized thrust faults, and
94 align with the micro-earthquake trends, but not with the NIFZ.
- 95 5. Large cross faults repeatedly offset the fold axis of the SBA, resulting in
96 compartmentalized and rotated fault blocks along the SBA axial strike, as
97 documented by well logs, production data, and 3D seismic data, and are analogous
98 to adjacent cross-faults documented offshore at Wilmington Anticline
99 (Ishutov,2013, Clark,1987, Wolfe, 2019). These large cross-faults which extend for
100 miles into the offshore are not easily explained by pure strike-slip tectonics.
- 101 6. The strong motion sensor at Long Beach (LBPU) recorded abnormally high vertical
102 acceleration with respect to the horizontal acceleration and are inconsistent with
103 horizontally-dominant strike-slip displacements that would be expected from the
104 NIFZ, and as predicted by recent NIFZ simulation models (Hough and Graves,2020).

- 105 7. Sediment cores taken within the Seal Beach Wetlands along the extrapolated NIFZ
106 surface trace documented recurring changes of depositional environments and
107 faunal communities associated with abrupt vertical elevation changes resulting
108 from coseismic events (Lepper,2017). However, despite the proximity of the cores
109 to the NIFZ, no analogous changes associated with the 1933 Long Beach
110 Earthquake were observed.
- 111 8. Modern 3D seismic data along the Seal Beach Anticline (SBA) reveals that faults
112 previously identified from oil well logs as NIFZ faults correlate to a complex sub-set
113 of antithetic faults along the SBA related to the previously unrecognized Garden
114 Grove Fault (GGF), which surfaces approximately 1-1 ½ miles (1.6 – 2.4 km) east of
115 the NIFZ (Biondi,2023). The GGF, an east verging listric thrust fault, is the dominant
116 fault creating and carrying the SBA.
- 117 9. The antithetic faults and SBA anticlinal folding terminate at a depth of
118 approximately 5500 feet (1675 m) subsea at the GGF decollement, rather than
119 continuing to basement as predicted by strike-slip theory, and terminate along
120 strike in both directions.



121
 122 Figure 1. Published structural contours and key faults associated with Wilmington Anticline and
 123 Signal Hill Anticline, and oil wells associated with Seal Beach oil fields (green dots). Dotted
 124 pink line indicates the currently mapped surface position of the NIFZ. Gold circles represent
 125 micro-earthquakes recorded by dense seismic networks. Area encompassed by 2017 3D survey
 126 highlighted in gray. Seal Beach Naval Weapons Station (SB NWS) is shown in lower right
 127 corner (yellow highlight). Yellow star on inset map indicates study location.

128

129 **2. Method: Integration of New Datasets**

130 In 2017, a proprietary high resolution 28 square mile (45 square km) 3D survey was
 131 acquired centered along the NIFZ and the Seal Beach Anticline, covering the area along
 132 strike between the southern end of Signal Hill Anticline and the Seal Beach Naval Weapons

133 Station, and extending in the dip direction about 1 mile (1.6 km) offshore along the east
134 flank of Wilmington Anticline to approximately six miles (9.7 km) onshore (Figure 1). This
135 high-resolution 3D dataset provides some of the most detailed subsurface information
136 presently available for direct analysis of faults and corresponding deformation, as well as
137 quantifying tectonically related stratigraphic features throughout the Seal Beach trend, and
138 for providing chronostratigraphic control for well log correlations.

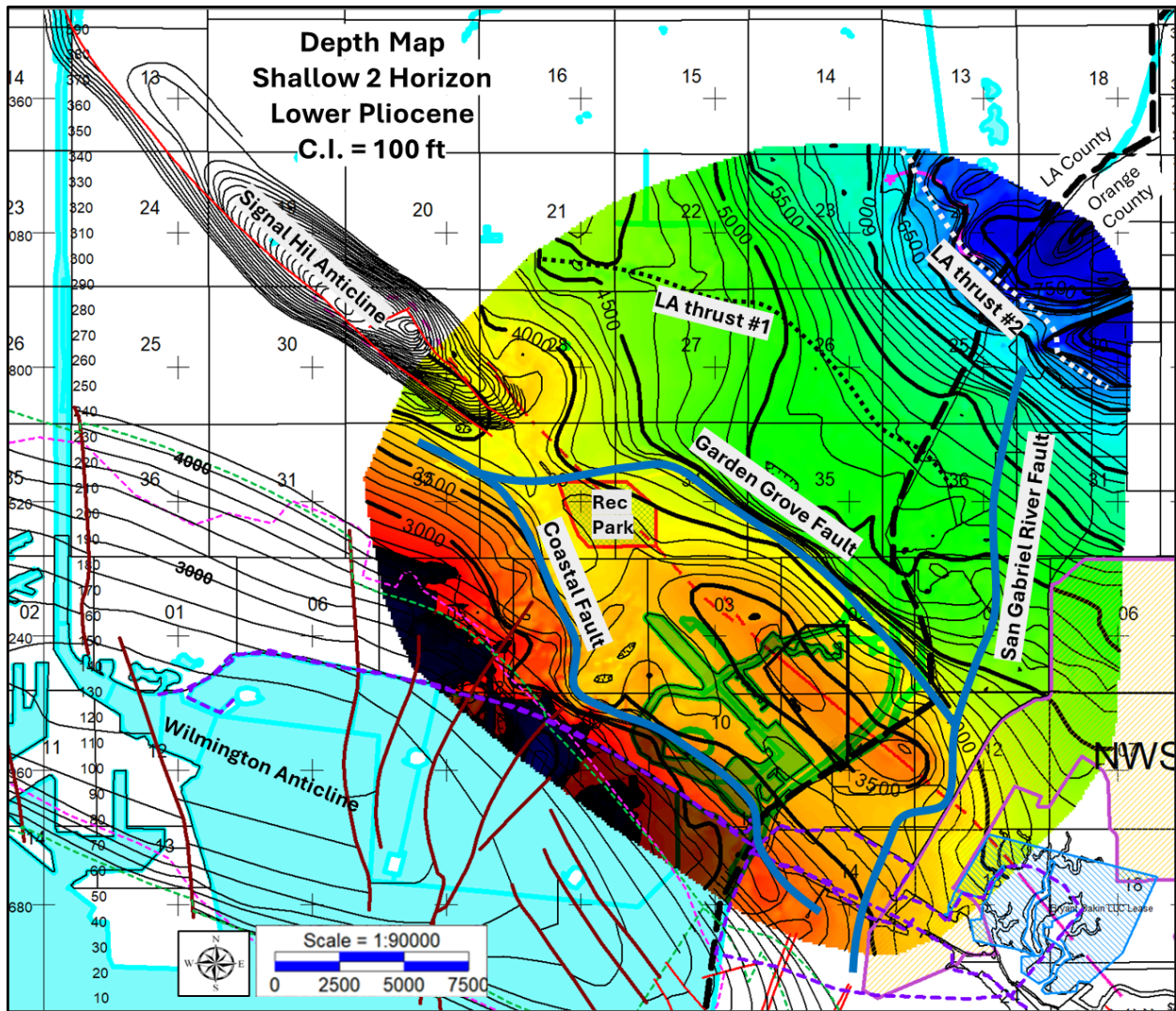
139 Integration of multiple 3D seismic attribute volumes assisted in providing data
140 redundancy and clarity to the interpretations. These multiple attribute volumes included
141 multiple PSTM datasets, enhanced impedance volumes, animated horizontal timeslice
142 volumes, integration of hundreds of oilfield well logs using proprietary log correlations and
143 formation tops tied to the 3D data, historical production data, logs from two new
144 proprietary oil wells, new proprietary check shot velocity surveys, correlations with
145 published structural and subsurface data from Wilmington Field tied along the western
146 edge of the 3D dataset, and with selected subsurface well data associated with the Long
147 Beach oil field. Regional 3D depth conversions were further assisted by proprietary
148 correlations between seismic inversion data and public and proprietary well logs, providing
149 a greater density of lateral and vertical control points to calibrate extensive velocity
150 anisotropy throughout the survey.

151 The passive 3D seismic dataset, analyzed by Caltech using autocorrelation techniques
152 to identify micro-earthquakes which occurred during the survey acquisition (Figure 1),
153 resulted in identifying more than 1200 high confidence nighttime events (Yang and
154 Clayton,2021). None of the 2017 micro-events registered on the Southern California

155 Seismic Network (SCSN) because the events occurred below the SCSN detection
156 threshold of M2.5. Geo-located coordinates (X-Y-Z) of the micro-earthquake epicenters
157 using independent velocity models developed by Caltech were incorporated into the depth
158 converted 3D seismic dataset. Epicenter locations were subsequently correlated with
159 faults interpreted on 3D seismic data.

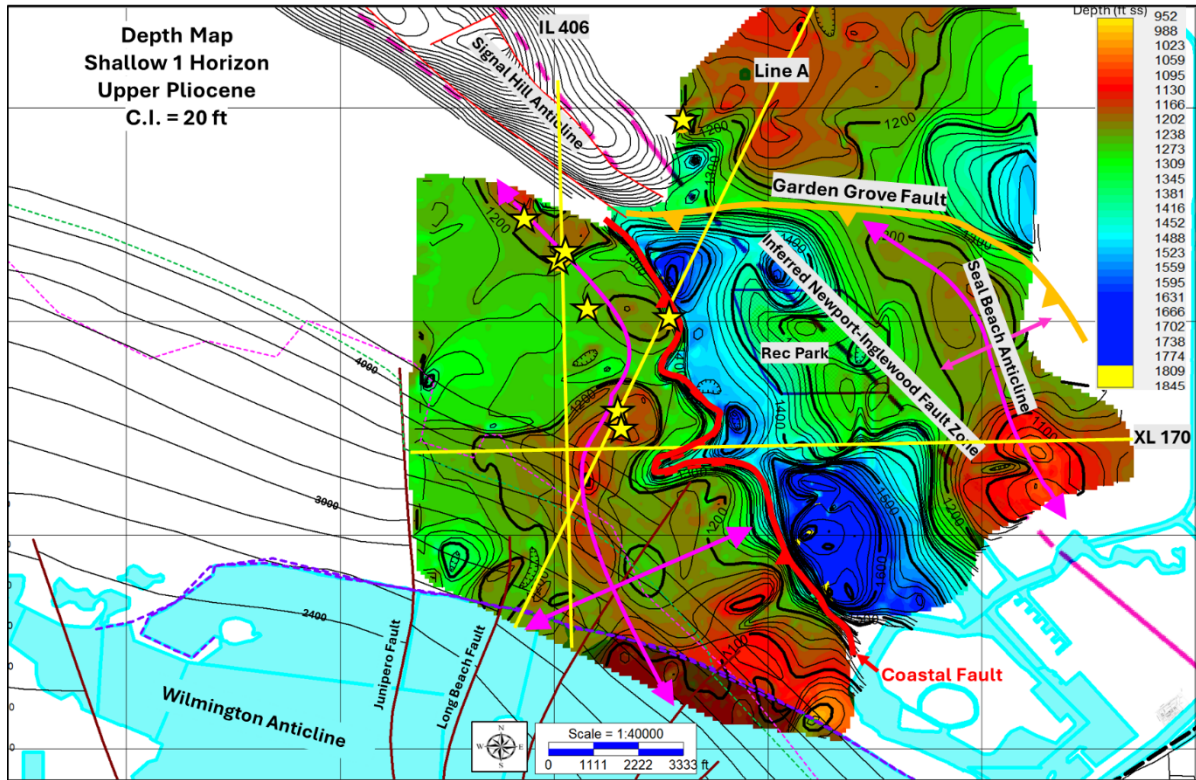
160 **3. Results/Observations**

161 The SBA is carried by the GGF thrust sheet, including dozens of antithetic faults related
162 to recurring deformation of this structure, which terminates immediately north of
163 Recreation Park and along strike to the south near the western edge of the Seal Beach
164 Wetlands, as a doubly terminated anticline (Figures 2 and 3).



165

166 Figure 2. Mapped Lower Pliocene horizon (Shallow2, green horizon in Figure 4) is ~1400 ft
167 above the Ranger Fm (Wilmington contours). Dashed red line shows the USGS surface trace of
168 NIFZ (Calif. Geol. Survey, 2024).



169

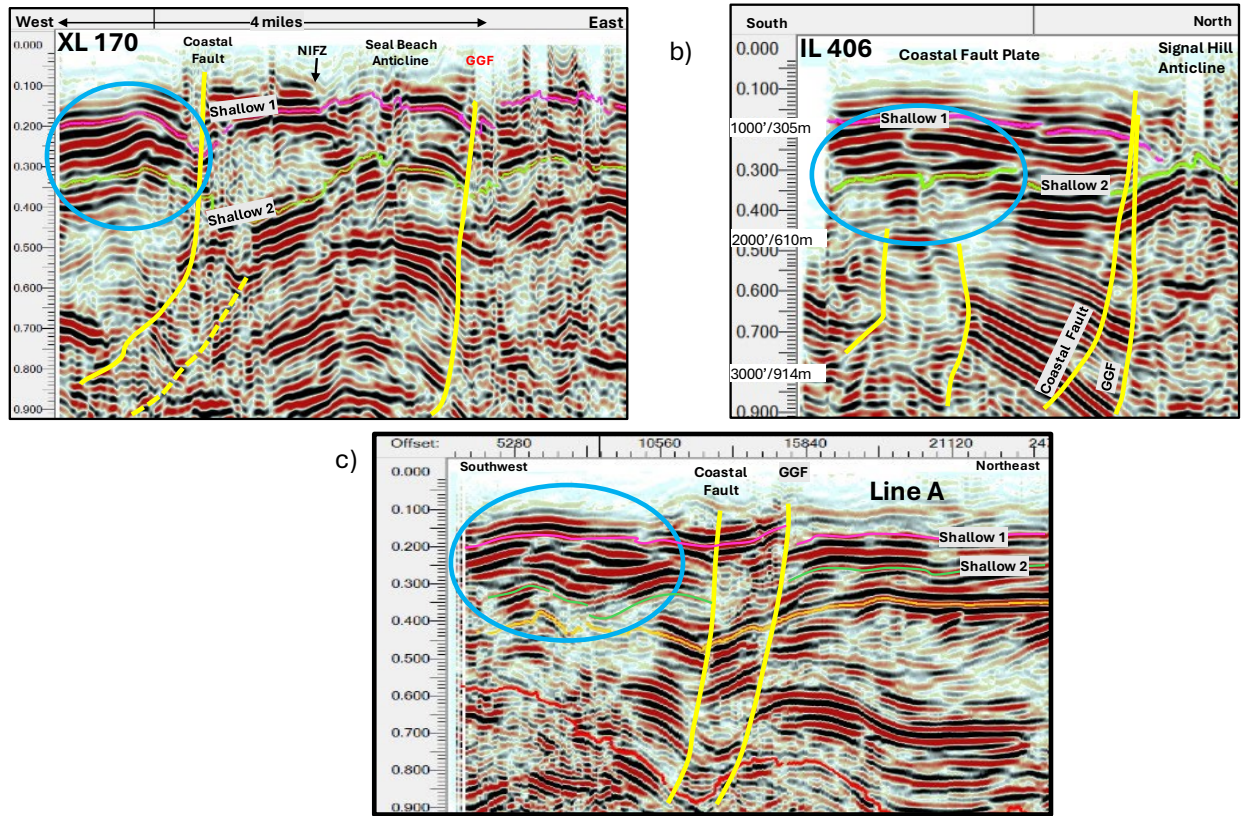
170 Figure 3. Structure map on the Upper Pliocene Shallow1 (pink) reflector shown in Figure 4.
 171 Seismic x-section lines in Figure 4 are shown as solid yellow lines. Pink arrows indicate strike
 172 and dip of anticlinal folding of Coastal Fault and Garden Grove thrust plates. Micro-
 173 earthquakes at the north end of the Coastal Plate (yellow stars) correlate with the leading edge of
 174 the Coastal Fault (solid red line). GGF shown by solid gold line. Note offset of SBA with
 175 respect to Signal Hill Anticline at shallow horizons. Lower left structural contours are mapped
 176 on the deeper Ranger Formation in Wilmington Field. Brown lines are named cross faults at
 177 Wilmington Oil Field. Signal Hill and Wilmington Anticline contours are from published maps.

178

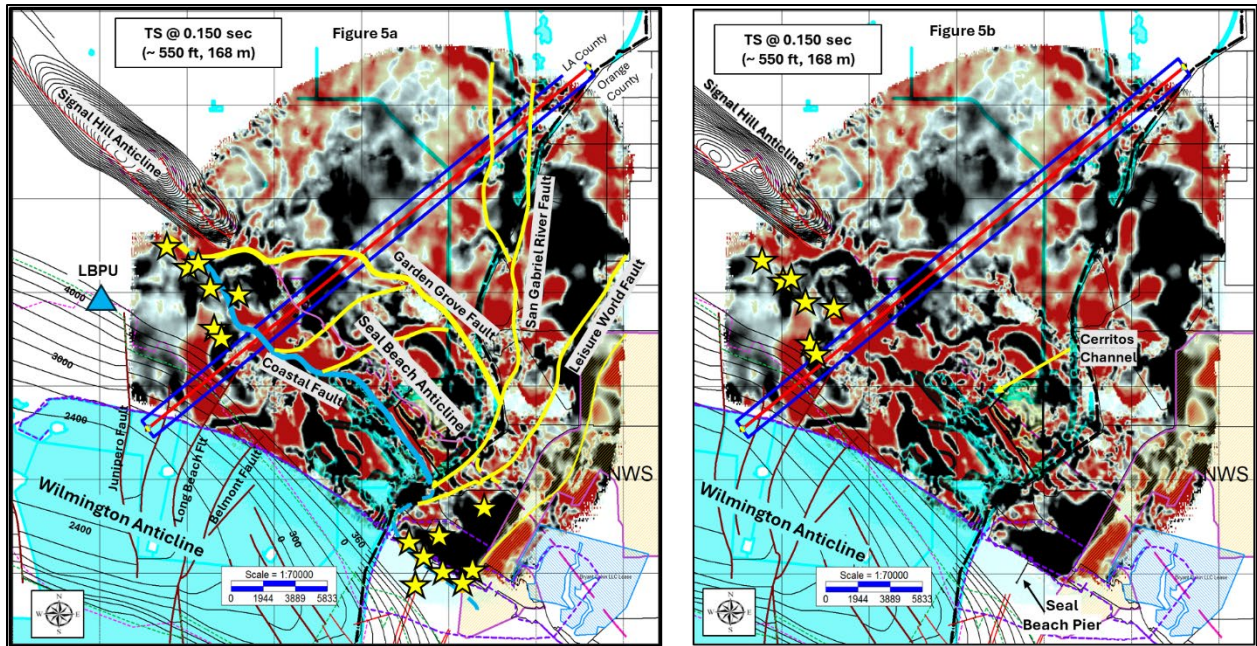
179 Additionally, the SBA fold and its antithetic faults are truncated by the GGF décollement at
 180 depths of approximately 5500 ft (1675 m) (Figures 6 and 7). The southern terminus of the
 181 SBA is offset by a series of closely spaced NE-SW trending faults, the San Gabriel River
 182 Fault and the Leisure World Fault, resulting in right-lateral offset of the SBA structural axis
 183 (Figure 5a).

184

185 The GGF is a listric fault (Figures 4, 6, and 7) which surfaces approximately 1 to 1.5
186 miles (1.6 to 2.4 km) northeast (Figure 5) of the NIFZ surface trace (Biondi,2023) and carries
187 the SBA as a ramp anticline within the leading edge of the GGF salient.



188
189 Figure 4. Coastal Fault with folding along leading edge of the thrust plate. Mapped horizons in
190 Figures 2 & 3 are shown in green and pink respectively; areas within blue circles show more
191 intense shallow thrusting than on other thrust plates.

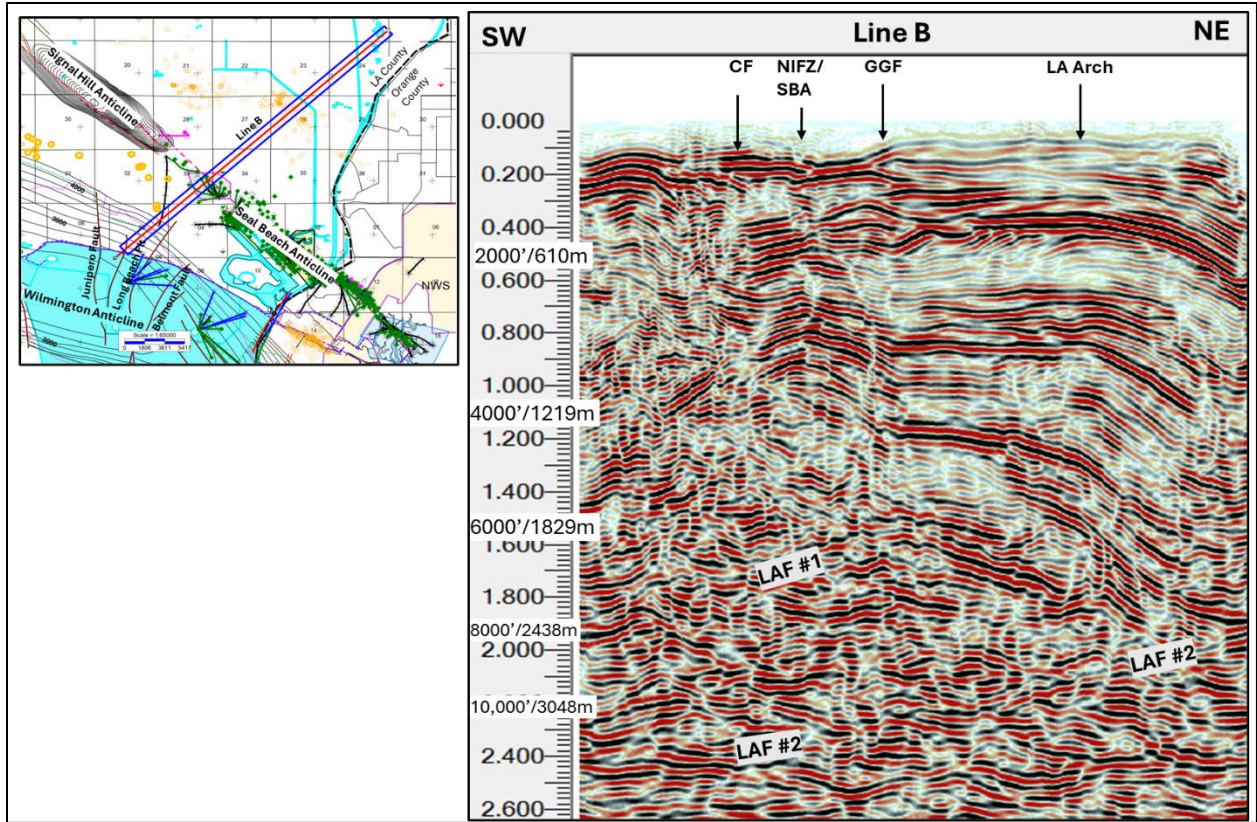


192

193 Figure 5. **5a**: Interpreted seismic amplitude timeslice at approximately 550 ft ss (168 m) Upper
 194 Pliocene, showing arcuate trace of the GGF (yellow line) cutting obliquely between Signal Hill
 195 Anticline and Seal Beach Anticline. Blue line is the Coastal Fault. Pink line is the NIFZ. **5b**:
 196 Uninterpreted timeslice. Seismic x-section (red line) is shown in Figure 6. Yellow stars are
 197 select micro-earthquakes recorded during 2017.

198

199 Below the GGF décollement, a previously unrecognized system of generally NW-SE
 200 oriented thrusts extend basinward as blind thrusts from nearly 1 mile (1.6 km) offshore
 201 along the east flank of Wilmington Anticline to at least six miles into the Los Angeles Basin,
 202 and are named the Los Alamitos Fault #1 (LAF #1), and the Los Alamitos Fault #2 (LAF #2),
 203 (Figures 2, 6, and 7).



204

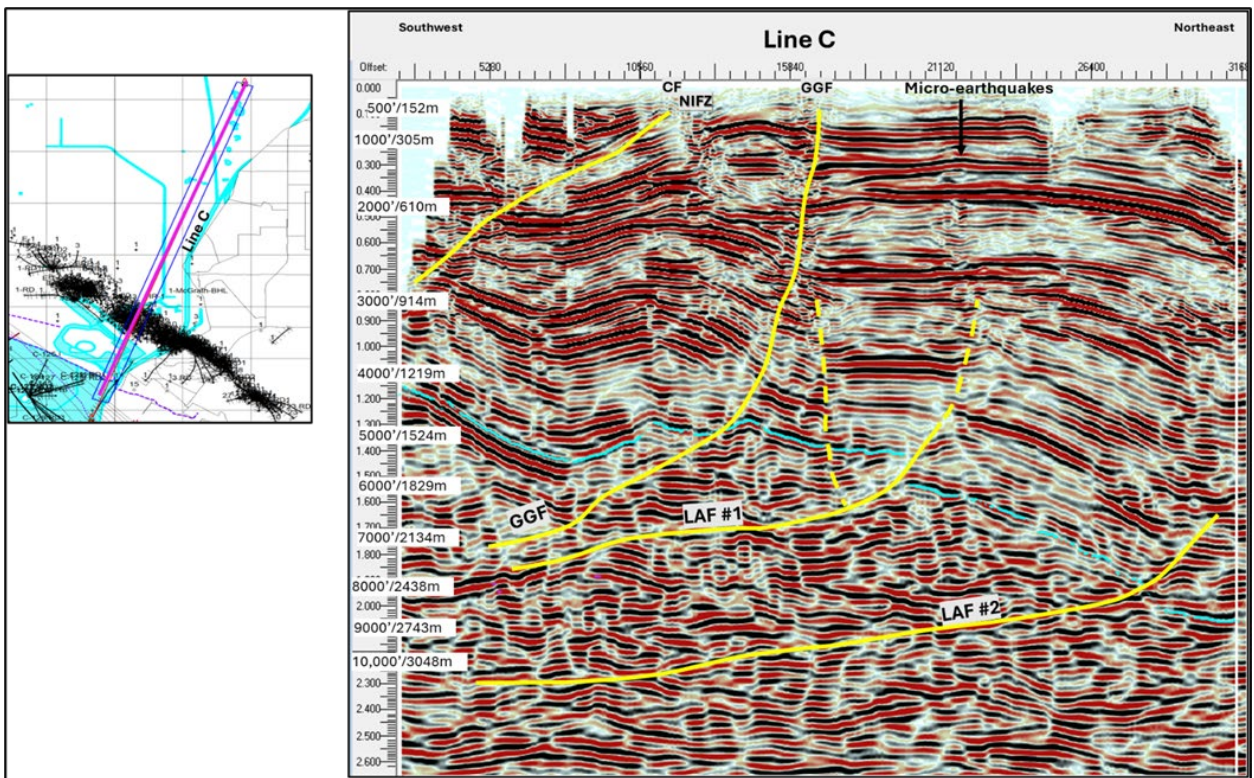
205 Figure 6. Uninterpreted diagonal seismic line through Recreation Park, with surface locations of
 206 major faults labeled. SBA does not exist below ~5500 ft (1675m), consistent with a thrust
 207 anticline. NIFZ neither extends to basement, nor dips eastward into the basin. The Coastal Fault
 208 (CF), plate (upper left corner) is tightly folded with a steeply dipping east flank. Underlying
 209 blind thrust faults occur at ~1.80 sec (LAF#1) and at ~2.4 sec (LAF#2) which steeply folds the
 210 northeast limb of the Los Alamitos Arch.

211

212 Tectonic deformation of shallow sediments is not restricted to just along the SBA trend.
 213 Seismic data shows intensely deformed shallow reflectors, characterized by tightly folded,
 214 thrust, and steeply dipping beds occurring several miles west of SBA along the coast,
 215 corresponding with a recently identified large thrust plate, the Coastal Fault (Figure 4).

216 Within the study area, thousands of feet of sediments were continuously deposited
 217 within relatively low energy fluvial-deltaic-lagoonal environments as essentially horizontal

218 sediments. However, 3D seismic data shows multiple high stand systems tracts (HST's)
219 stacked along the eastern, downthrown side of the Garden Grove Fault (Figures 4c, 6, and
220 7), indicating repeated uplift of the GGF fault block creating corresponding updip
221 accommodation spaces; yet no similar HST's were observed along the NIFZ. Sequence
222 stratigraphy analysis of these parasequences record up to 1000 feet (305 m) of recurring
223 vertical displacements of the GGF during the Upper Pliocene through Upper Pleistocene,
224 based on the combined vertical separation between "topset" and "toeset" reflections.



225
226 Figure 7. Garden Grove Fault carries the Seal Beach Anticline as a ramp anticline, which
227 disappears below ~5500 feet (~1,680 m) at 1.50 sec. The NIFZ neither extends to basement
228 nor dips eastward into the basin. Basement is interpreted to occur below 2.6 seconds.
229 Horizontal scale (feet) shown across top of section.

230

231 Hundreds of micro-earthquakes recorded in 2017 (Figure 1) by a dense seismic network
232 have been directly tied to the Coastal Fault, and to the Los Alamitos #1 blind thrust,
233 indicating these faults remain active today. The widely spaced occurrence of these micro-
234 earthquakes are consistent with the widely spaced aftershocks following the 1933 Long
235 Beach Earthquake. Virtually all the recent micro-earthquakes recorded south of Signal Hill
236 occurred along the flanks of the Seal Beach Anticline rather than along the projected NIFZ
237 trace (Yang and Clayton,2021).

238 **3.1 Coastal Fault newly discovered**

239 Steeply east-dipping sediments paralleling the coastline between the coast and Seal
240 Beach Anticline are folded and carried by an east-vergent thrust fault, herein called the
241 Coastal Fault (Figure 2 and 3). The Coastal Fault (CF) flattens offshore toward the west,
242 based on observations that i) hanging wall structures exhibit listric anticlinal folding along
243 the leading edge (Figures 4, 6 and 7), ii) steeply dipping horizons along the eastern flank of
244 the thrust sheet terminate abruptly against flatter footwall horizons (Figures 4 and 6), and
245 iii) cutoff positions of hanging wall horizons move progressively westward with increasing
246 depth, at least down to mid Miocene horizons. Seismic data along the Coastal Fault thrust
247 sheet reveals thrust faulting of even very shallow sediments (Figure 4) and pronounced
248 folding along the leading edge of the Coastal Thrust plate on the east flank of Wilmington
249 Anticline, consistent with the transpressive thrust structure proposed for Wilmington
250 Anticline (Ishutov,2013). The Coastal Fault exhibits up to 200 – 250 feet (61 – 76 m) of
251 vertical displacement (Figure 3) of Upper Pliocene sediments west of Recreation Park and
252 extends southward sub-parallel to the coastline, passing under the Marina area. Near the

253 Seal Beach Pier, the CF also correlates with a fault segment about 1 mile (1.6 km)
254 southwest of the NIFZ which is associated with recent micro-seismic activity (Clayton and
255 Yang,2021, Yang and Clayton,2021), proving it remains active.

256 The Coastal Fault and the Garden Grove Fault appear to merge south of Signal Hill
257 representing a large northeast-vergent thrust salient (Figure 5) carrying the SBA between
258 Signal Hill and the western edge of the Seal Beach Wetlands. Where the two faults merge
259 west of Recreation Park (Figures 2, 3), the combined Garden Grove Thrust and the Coastal
260 Thrust are interpreted to have east-west oriented, left-lateral transpression relative to the
261 northern block carrying the Signal Hill Anticline, consistent with oblique thrusting, rather
262 than NW-SE oriented right-lateral strike slip displacement.

263 **3.2 Micro-earthquakes reveal new fault zones**

264 The dense 3D geophone network installed during the 3D seismic acquisition period
265 continuously recorded data over a three (3) month period, resulting in two distinct
266 datasets, one which recorded dynamic reflection energies, and a second passive dataset
267 which recorded only ambient energies. The passive dataset was delivered to Caltech who
268 identified more than 1200 high-confidence micro-earthquakes having magnitudes less
269 than M2.5, none of which registered on the Southern California Seismic Network because
270 they were below the networks' detection threshold (Clayton and Yang,2021). These micro-
271 earthquakes aligned in distinct patterns across the survey, revealing new clues as to
272 locations of previously unrecognized faults, and of current seismic activity levels (Yang and
273 Clayton,2021). Significantly, none of the recent micro-earthquake epicenters aligned with

274 the NIFZ south of Signal Hill (Figure 1). Most events were oriented along a NW-SE trend
275 located approximately 2 miles (3.2 km) north of NIFZ, correlated with the leading edge of
276 the Los Alamitos #1 Thrust, a blind thrust. A second dense cluster of events occurred at
277 the shoreline near the Seal Beach pier (Yang and Clayton, 2021) more than a mile from
278 NIFZ. No events were detected along the NIFZ.

279 A third cluster of micro-events were recorded along a NW-SE trend ½ mile (0.8 km)
280 south of Signal Hill Anticline and are clearly offset from the NIFZ (Figures 1, 3, and 5). The
281 location and orientation of these micro-events correlate with the northern extent of the
282 Coastal Fault plate along its leading edge. The micro-earthquake cluster south of Signal
283 Hill Anticline and the cluster near Seal Beach pier, as well as shallow deformation
284 documented by 3D seismic data, confirm that the Coastal Fault is presently active. This
285 deformation is characterized by extensive shallow thrusting, and tightly folded, steeply
286 dipping Pliocene sediments offsetting the Seal Beach Anticline and the NIFZ by 1.5 - 2
287 miles (2.4 – 3.2 km) (Figures 4, and 6).

288 3.3 Newport-Inglewood Fault Zone

289 Detailed mapping of NIFZ faults along Seal Beach Anticline indicates NIFZ faults
290 have frequently been correlated to numerous relatively minor en-echelon antithetic faults
291 related to the Garden Grove thrust. These en-echelon fault segments lack significant
292 displacement, neither vertically nor horizontally, and do not follow the strike of the NIFZ
293 surface maps but have been locally rotated clockwise due to cross faulting, resulting in
294 local north-south orientations (Gish and Boljen, 2015).

295 It is worth repeating that the Seal Beach Anticline, historically interpreted as a major
296 structural anticline related to dextral strike slip faulting along the NIFZ, and as a southern
297 continuation of the Signal Hill Anticline, in this 3D seismic dataset: i) is carried by the GGF
298 thrust salient, ii) disappears entirely below the Garden Grove decollement at ~5500 feet ss
299 (-1524 m), iii) folding along the SBA terminates in both directions along strike resulting in a
300 doubly plunging anticline approximately 4 miles (6.4 m) long, iv) the asymmetrical SBA fold
301 axis is displaced to the east of Signal Hill Anticline by left lateral faulting at shallow
302 Pliocene horizons but aligns with it at deeper Lower Pliocene horizons (Figures 2 and 3), v)
303 the fold axis of the anticline dips westward as the anticline deepens, vi) the SBA fold axis is
304 repeatedly offset by cross-faults which can be correlated to well documented cross faults
305 at Wilmington Anticline, vii) the mapped surface location of the NIFZ at Recreation Park
306 occurs significantly off-structure along the west flank of the SBA at Upper Pliocene
307 reflectors (Figure 3, and 4c), and viii) none of the ~1200 high confidence micro-earthquakes
308 recorded in 2017 correlate to NIFZ faults along SBA (Figure 1). These facts do not support
309 the classic definition of the NIFZ as a regionally extensive, narrow-width, near vertical,
310 basement-related, strike-slip fault.

311 **4. Discussion**

312 The 2017 micro-seismic activity which is correlated to a widely spaced system of thrust
313 faults on both sides of the SBA suggests these faults are linked at depth, complexly
314 interacting via a displacement mechanism which is distinctly different from that of the NIFZ
315 strike slip focal mechanism solution recorded at its Huntington Beach epicenter, which has

316 historically been associated with the 1933 Long Beach Earthquake and subsequently
317 extrapolated along the inferred NIFZ trace.

318 This paper does not take issue with the interpretation of the fault plane solution
319 assigned to the 1933 Long Beach Earthquake near Huntington Beach (Haucksson and
320 Gross, 1991), but rather with the manner in which subsequent rupture has been assumed
321 to propagate exclusively along a narrow fault zone, the NIFZ, as essentially pure strike-slip
322 displacement throughout the Seal Beach area and into Long Beach. It is not necessarily
323 true that subsequent propagation of the rupture process can or should be associated with
324 a single unique fault. Continued efforts to extrapolate focal mechanism results obtained at
325 the Huntington Beach epicenter to deformation observed at Long Beach have proven to be
326 less than satisfactory. Considerable conflicting evidence indicating that a different
327 tectonic regime is active within the Seal Beach area has been largely ignored and discarded
328 in favor of traditional NIFZ models. The 2017 micro-earthquake results, recognition of the
329 GGF thrust plate carrying SBA, extensive shallow deformation observed on 3D seismic
330 data throughout the study area, atypical displacement parameters recorded by the LBPU
331 instrument during the 1933 Long Beach Earthquake, and active thrust faults extending into
332 the Los Angeles Basin under SBA are consistent with the nearly 10 miles wide (17 km)
333 onshore aftershock pattern which occurred during the 1933 Long Beach Earthquake
334 (Haucksson and Gross 1991), and with the compressional tectonic system and significant
335 cross-faulting described at Wilmington Anticline (Ishutov, 2013), Clark, 1987, Wolfe 2019,
336 Wright 1991, Ponti 2007).

337 Micro-earthquake activity throughout Seal Beach is associated with a system of
338 thrust sheets extending eastward from the Wilmington Anticline, that have been
339 subsequently displaced by well documented cross faults cutting the Wilmington Anticline
340 which can be extended onshore at least to the leading edge of GGF. The SBA cross faults
341 are primarily concentrated near the change of strike of the thrust salient immediately south
342 of the Signal Hill Anticline, near Recreation Park, but also cut SBA ½ mile (0.8 km) north of
343 Cerritos Channel as a very apparent offset likely associated with the Belmont Fault cross
344 fault (Figure 5). Evidence of recent deformation is particularly evident west of Recreation
345 Park, along the Coastal Fault plate where the GGF merges with the Coastal Fault,
346 coinciding with the area of extreme deformation and anomalous intensities observed
347 during the 1933 Long Beach Earthquake (Figures 3 and 4).

348 These newly identified structural details imply that a wide transpressional tectonic
349 system has been prevalent from Mid Pliocene to Recent times within the study area, in
350 contrast to long-held beliefs of dextral strike slip displacement focused along a narrow,
351 near-vertically oriented fault (NIFZ) along the Seal Beach Anticline. SBA is not simply a
352 continuation of Signal Hill faulting and folding extending to basement and striking
353 southeastward into the Wetlands areas, but rather is restricted to the GGF thrust plate.
354 Within the study area, new seismic evidence shows the NIFZ does not exist as a
355 meaningful, competent fault system, and that other major faults and pre-existing structural
356 elements are transferring and propagating unique energy wavefields, resulting in atypical
357 intensity distributions and localized ground motion amplification.

358 Detailed measurements of large rupture events in Ecuador (Chalumeau, C.,2024)
359 using highly sensitive dense arrays, and in California (Lee, J.,2024), have shown that
360 regional displacement transfer is not necessarily restricted to a single fault type, nor to a
361 single fault zone or geometry type, but can occur between different fault blocks due to
362 deep-seated structural linkage and pre-existing fault networks, resulting in considerable
363 variations of local dispersion kinematics as energy propagates along strike.

364 The apparent change in displacement transfer mechanism from pure strike-slip
365 near the Huntington Beach epicenter to transpressional displacements along an active
366 thrust fault trend at Seal Beach helps to explain the unusually extreme vertical acceleration
367 values recorded by LBPU miles away from the NIFZ, and why efforts to model that data
368 based solely on NIFZ strike-slip models have consistently under-predicted observed
369 results.

370 This paper proposes that a complex system of linked east-vergent thrust faults may
371 have transformed initial NW-SE oriented dextral strike-slip displacements recorded at the
372 Huntington Beach epicenter into transpressional displacements between Signal Hill
373 Anticline and Seal Beach Wetlands, primarily accommodated by the Coastal Fault, Garden
374 Grove Fault, and Los Alamitos Thrust #1. The point at which this change in displacement
375 mechanism occurs may coincide with an enigmatic NE-SW trending fault zone, the San
376 Gabriel River and Leisure World faults zone (SGR/LWF) (Figures 2 and 5). These large,
377 extensive faults displace the SBA with dextral offset near the western edge of the Seal
378 Beach Wetlands and extend northward beyond the 3D dataset with generally down-to-the-

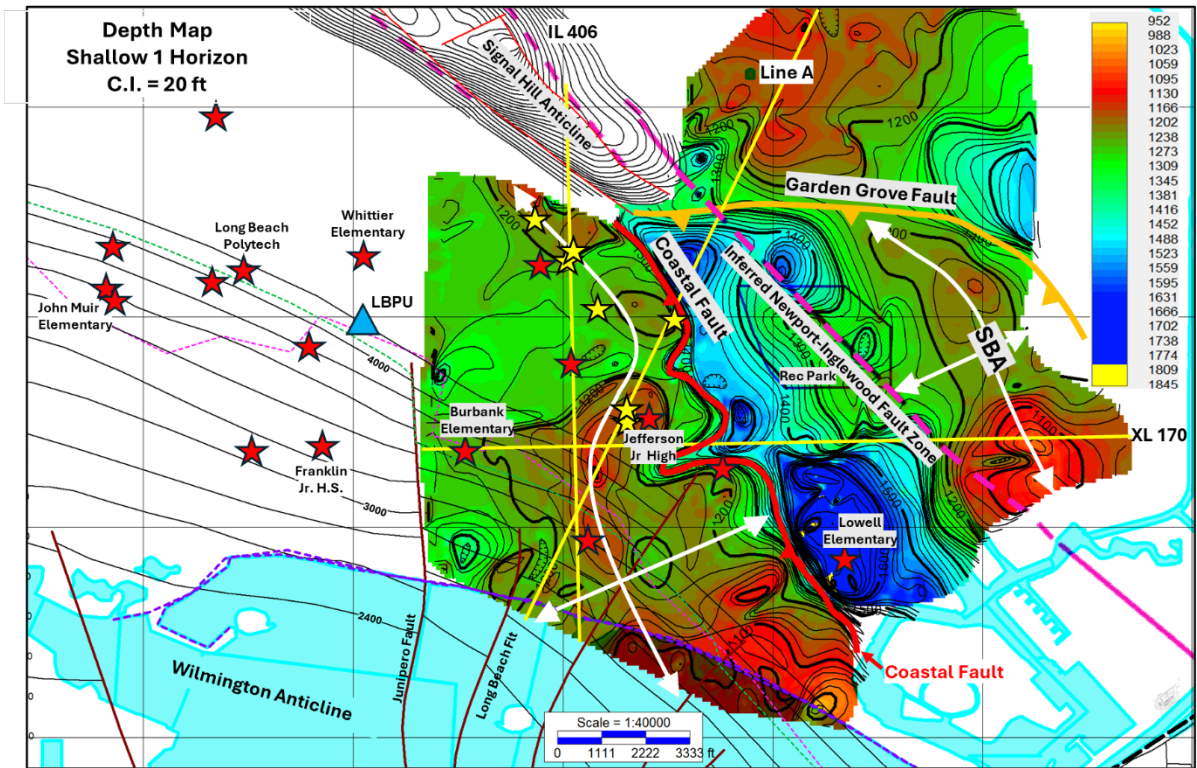
379 east displacement. North-south oriented folding of recent sediments along the SGR/LWF
380 zone indicates the faults are currently active.

381 During the 1933 Long Beach Earthquake, the strong motion instrument, LBPU,
382 recorded ground acceleration values of 0.20g, 0.16g and 0.29g for north-south horizontal,
383 east-west horizontal, and vertical displacement components, respectively. While there
384 may have been some instrument saturation of the horizontal components at peak ground
385 acceleration rates, the vertical acceleration component is deemed reliable (Hough and
386 Blair, 2023). One of the most striking observations from these data is that the vertical
387 displacement component at LBPU exceeds the maximum horizontal component by a ratio
388 of 1:1.45. These results are in surprising contrast to the expected response from “pure
389 dextral strike-slip” as determined by Haucksson and Gross (1991) for the epicentral rupture
390 mechanism near Huntington Beach. The extreme ground acceleration and anomalous
391 vertical displacement values recorded by LBPU are not easily explained by efforts to assign
392 the 1933 Long Beach response parameters exclusively to the NIFZ, located about 3 miles (5
393 km) away. Additionally, a more complex rupture scenario supporting two distinct
394 propagation sub-events (“asperities”) near Long Beach was noted by Haucksson and Gross
395 (1991). The northernmost of the two asperities was calculated to be about 3.7 – 4.3 miles
396 (6 – 7 km) in length, a distance and location that agrees very well with the width of the
397 Coastal Fault-GGF salient.

398 Recent earthquake simulations using an extended length NIFZ rupture model
399 resulted in predicted maximum horizontal acceleration of 0.35g and vertical acceleration
400 of 0.09g, less than 1/3 the observed vertical acceleration value recorded at LBPU, and a

401 relative vertical:horizontal ratio of just 0.26 (Hough and Blair,2023). While the modeled
402 displacement ratio is consistent with nearly pure strike-slip displacement mechanisms as
403 expected, it vastly under-predicts the observed vertical displacement ratio of 1:1.45 which
404 was recorded by the LBPU strong motion instrument. While it is possible the horizontal
405 components of LBPU were saturated at the highest acceleration rates and that greater
406 horizontal displacement values may have resulted in a lower vertical:horizontal
407 displacement ratio for the 1933 earthquake, achieving the vertical:horizontal displacement
408 ratio of 0.26 predicted by extended rupture simulations would require the horizontal
409 displacement at LBPU to have reached a maximum value of 1.1g, in contrast to the actual
410 recorded LBPU value of 0.20g, or even the modeled maximum horizontal value of 0.35g.
411 Considering that no surface ruptures were observed at Long Beach nor along the NIFZ, this
412 possibility seems unlikely. Instead, it is more likely that the anomalous 1933 Long Beach
413 rupture kinematics observed near Long Beach occurred in response to a different tectonic
414 mechanism than that of the strike-slip event recorded at Huntington Beach.

415 Locations of well documented collapsed school buildings and of the LBPU strong
416 motion instrument from the 1933 Earthquake, and micro-earthquake locations recorded
417 during the 2017 survey have been superimposed on an Upper Pliocene 3D seismic
418 structure map (Figure 8). Although the 3D Seal Beach survey does not extend far enough
419 west to fully image the entire area of Long Beach damage, a strong correlation can be made
420 between recent deformation along the Coastal Plate and documented evidence from the
421 1933 Long Beach Earthquake.



422

423 Figure 8. Map shown in Figure 3 with superimposed locations of Long Beach collapsed
 424 school buildings (red stars) and seismometer LBPB (blue triangle). Yellow stars show
 425 select 2017 micro-earthquake locations. Brown lines are known cross faults at Wilmington
 426 Field. Yellow lines are seismic lines shown in Figure 4.

427

428 The lack of sedimentary response to the 1933 Long Beach Earthquake documented
 429 by shallow core data within the Seal Beach Wetlands (Lepper, 2017) implies that the NIFZ
 430 was not involved in the 1933 rupture mechanics at least at this location, and that perhaps
 431 displacement transfer from the NIFZ to the Coastal Fault, and to the underlying thrusts
 432 occurred upon encountering the San Gabriel/Leisure World Fault zone, the second
 433 “asperity” reported by Haucksson and Groves (1991).

434 This new tectonic model proposes that displacements from the 1933 Earthquake
 435 which originated at an epicenter 15 miles (25 km) to the south and offshore from

436 Huntington Beach as pure strike slip rupture along the NIFZ, may have been subsequently
437 transferred to the pre-existing Coastal/Garden Grove/Los Alamitos thrust sheets during
438 northwest propagation. The location of the suggested transfer zone is proposed to occur
439 along the San Gabriel/Leisure World Fault zone (Figure 5). Transpressional displacement of
440 the Coastal Fault plate, perhaps amplified by contributions from the GGF rather than
441 strike-slip displacement along the NIFZ, was most likely responsible for the anomalously
442 high ground acceleration values, high vertical displacement ratios, and extreme intensities
443 experienced at Long Beach during the 1933 Long Beach Earthquake event. Such a
444 modified rupture mechanism is consistent with the two-stage propagation scenario
445 discussed by Haucksson and Groves (1991).

446 **5. Conclusions**

447 High resolution 3D seismic data has revealed previously unrecognized thrust faults
448 within the Seal Beach area, associated with intense near-surface deformation and with
449 micro-earthquake patterns recorded by dense seismic networks during 2017 along both
450 flanks of the SBA, but not along the NIFZ. Within the greater Seal Beach area there is little
451 evidence supporting the concept of a large regional strike-slip fault system corresponding
452 to assumed NIFZ models. Faults previously described as NIFZ faults are identified as
453 numerous antithetic fault segments associated with leading edge deformation. The
454 doubly-plunging Seal Beach Anticline is carried as a ramp anticline by the Garden Grove
455 Fault, a previously unknown thrust fault which outcrops ~1.5 miles (2.4 km) east of the
456 NIFZ. SBA is separated from Wilmington Anticline on its west flank by the Coastal Fault,
457 another previously unrecognized thrust fault. Both faults are listric and flatten toward the

458 west. These distinctive thrust faults indicate that a transpressive tectonic regime rather
459 than a simple strike-slip tectonic system prevails within the Seal Beach region, identical to
460 the transpressional system described for the adjacent Wilmington Anticline. Dozens of
461 micro-earthquakes clustered along the Coastal Fault indicate the fault remains active,
462 whereas no corresponding events were detected along the NIFZ.

463 Previous researchers have reported that the 1933 Long Beach Earthquake
464 propagated toward the northwest from the Huntington Beach epicenter in at least two
465 discrete sub-events, or asperities, lending support to the concept presented in this paper
466 that propagation of the 1933 Long Beach Earthquake event may have begun as pure dextral
467 displacement at the initial source location near Huntington Beach, but transformed into
468 more complex transpressional displacements as the stress field encountered and
469 reactivated pre-existing thrust faults bracketing the Seal Beach Anticline area. One of
470 these previously unknown thrust faults, the Coastal Fault, closely parallels the coastline,
471 transforming the eastern flank of the Wilmington Anticline from simple east dip separated
472 from the SBA into a more complex structure crossing multiple thrust sheets. 3D seismic
473 data shows more intensive recent deformation along the Coastal Fault plate than along the
474 GGF plate or elsewhere, characterized by tight shallow folds and thrusts and hundreds of
475 recent microearthquakes, indicating that within the Seal Beach area, the CF is a dominant
476 fault more active than either the NIFZ or the GGF. The Coastal Fault merges with the
477 Garden Grove Fault immediately northwest of Recreation Park, effectively separating Signal
478 Hill Anticline from Seal Beach Anticline by west-east oriented, predominantly left lateral
479 faults corresponding to the edge of the CF/GGF salient. The combined displacements of

480 the merged faults may have been responsible for the amplified intensities and anomalous
481 accelerations observed at Long Beach. Abnormally high vertical accelerations recorded by
482 the LBPU instrument during the 1933 Long Beach Earthquake supports the interpretation of
483 transpressional displacement of the Coast Fault, resulting in larger vertical components
484 than would be expected from strike-slip rupture along the NIFZ. Similar dramatic changes
485 in rupture mechanics during large earthquakes have been documented by dense network
486 recordings in Ecuador.

487 More than 1200 high-confidence micro-earthquakes recorded in 2017 along distinct
488 trends flanking the SBA support the interpretation of an active, linked, widely dispersed
489 thrust system within the Seal Beach area of investigation. Linear swarms of shallow micro-
490 earthquakes recorded near the Seal Beach Pier and micro-events directly under Long
491 Beach corresponding to the Coastal Fault, combined with 3D seismic evidence of intense
492 shallow deformation, indicate the Coastal Fault has been and remains highly active. A
493 larger cluster of NW-SE trending micro-earthquakes located about 2 – 2.5 miles (~3.2 - 4
494 km) northeast of the GGF correlates with a near vertical fault zone along the leading edge
495 of a deep seated, previously unrecognized blind thrust, the Los Alamitos Thrust #1. An
496 even deeper blind thrust also correlated to deep micro-earthquakes, the Los Alamitos
497 Thrust #2, disappears into the basin beyond the northern limit of the 3D dataset. Los
498 Alamitos Thrust #2 is also uplifting and steeply folding the east flank of the Los Alamitos
499 Arch. The compelling evidence for widespread on-going activity over a width of nearly 6
500 miles (9.7 km) strongly suggests the thrusts may be linked in the subsurface.

501 The NIFZ is located approximately 1.5 - 2 miles (2.4 – 3.2 km) east of the area of the
502 most intense Long Beach ground shaking where more than 70 buildings were seriously
503 damaged and the LBPU strong motion instrument recorded extreme vertical acceleration
504 components that have not been satisfactorily explained by NIFZ model simulations.
505 Recent modeling of extended NIFZ rupture scenarios continue to under-predict the
506 observed vertical accelerations documented by the LBPU strong motion instrument by a
507 factor of more than three and does not explain recent micro-earthquake activity located
508 miles away on either side of NIFZ, but lacking along the NIFZ. Multiple antithetic faults
509 previously assumed to be NIFZ faults are spatially confined to the GGF thrust plate, are
510 highly compartmentalized by cross faults, and are not continuous either vertically or
511 horizontally. Structural and sedimentological data show that the GGF is a more dominant
512 fault than any of the antithetic faults associated with the SBA.

513 This study using integrated subsurface data proposes that anomalous Long Beach
514 surface damages and unusual ground motion parameters recorded by the LBPU strong
515 motion instrument can be better explained by transpressional rupture along the Coastal
516 Fault thrust plate, and perhaps the GGF plate, than by large strike slip movements along
517 the NIFZ.

518 Exactly where and how the transition from dextral strike-slip displacement along
519 the NIFZ near Huntington Beach to wide-spread transpressional fault system across a 6
520 mile wide thrust zone (Coastal Fault, Garden Grove Fault, Los Alamitos Faults #1 and #2) is
521 not entirely clear; however, 3D seismic data shows that a dramatic change in tectonic style
522 occurs along a NE-SW trending fault zone, the SGR/LW fault zone, oriented perpendicular

523 to the NIFZ approximately along the western boundary of the Seal Beach Wetlands which
524 may indicate a deep-seated transform boundary and correlate with the northernmost
525 asperity of the 1933 Earthquake. This enigmatic fault zone truncates the SBA at its
526 southern terminus, cuts and folds sediments less than 300 feet below the surface at the
527 Los Alamitos Arch and may also be associated with a right-stepping shear zone extending
528 into the offshore.

529

530 **Acknowledgements**

531 The Authors wish to provide thanks to Synergy Oil & Gas for permission to publish these
532 results, and to LA Seismic for acquiring and permitting the challenging field operations.

533 Thanks also go to continuing cooperation and constructive technical discussions with Dr
534 R. Clayton at Caltech.

535

536 **Data Availability**

537 The strong-motion data from three stations can be downloaded from:

538 <https://www.strongmotioncenter.org/cgi->

539 [bin/CESMD/iqr_dist_DM2.pl?IQRID=LongBeach_10Mar1933&SFlag=0&Flag=3.](https://www.strongmotioncenter.org/cgi-bin/CESMD/iqr_dist_DM2.pl?IQRID=LongBeach_10Mar1933&SFlag=0&Flag=3)

540 Micro-seismic data from the Long Beach-Seal Beach relocated nighttime seismicity
541 catalog can be found in the following Caltech repository:

542 <https://data.caltech.edu/records/5ws5e-ddh43>.

543 All websites were last accessed in November 2024.

544 Seismic reflection data was designed and collected for specific commercial purposes, is
545 considered proprietary data and is currently under corporate non-disclosure agreement.
546 3D Seismic Solutions has received permission to publicly display illustrations of the data
547 but may not make the actual digital data available.

548

549 **Competing Interests**

550 The authors declare there are no competing interests.

551

552 **References**

553 Biondi, E., Castellanos, J., Clayton, R., (2024) Imaging Urban Hidden Faults with Ambient
554 Noise Recorded by Dense Seismic Arrays, Seismological Research Letters

555 <https://doi.org/10.1785/0220230408>

556 California Geological Survey, California Department of Conservation, Seismic Hazards
557 Program, Earthstar Geographics, accessed January 16, 2024,

558 <https://maps.conservation.ca.gov/cgs/EQZApp/app/>

559 Clayton, R., and Yang, Y., Hollis, D., Gish, D., Boljen S. Campbell, E. and Stanford, B.

560 (2021) Results From 2017-18 High-Density Seismic Hazard Survey.

561 http://laseismic.com/2017-18_High-Density_Seismic_Hazard_Survey.ppsx

562 Chalumeau, C. Agurto-Detzel, H., Rietbrock, A., Frietsch, M., Oncken, O., Segovia, M.,
563 Galve, A., (2024) Seismological Evidence for a multifault network at the subduction
564 interface, *Nature*, Vol 628. <https://doi.org/10.1038/s41586-024-07245-y>

565 Gish, D., and Boljen, S. (2021) Newly Identified Fault in Seal Beach, CA, Quietly Rattles
566 Beneath the City, TK, *Temblor*, [https://temblor.net/earthquake-insights/newly-identified-](https://temblor.net/earthquake-insights/newly-identified-fault-in-seal-beach-ca-quietly-rattles-beneath-the-city-13477/)
567 [fault-in-seal-beach-ca-quietly-rattles-beneath-the-city-13477/](https://temblor.net/earthquake-insights/newly-identified-fault-in-seal-beach-ca-quietly-rattles-beneath-the-city-13477/)
568 <http://doi.org/10.32858/temblor.219>

569 Hauksson, E., Gross, S. (1991) Source Parameters of the 1933 Long Beach Earthquake
570 *Bulletin of the Seismological Society of America* 81 (1): 81–98.
571 <https://doi.org/10.1785/BSSA0810010081>

572 Hough, S. E., L. Blair, S. Ellison, R. W. Graves, S. Haefner, E. M. Thompson, N. van der Elst,
573 M. Page, and D. J. Wald (2023) Modern Products for a Vintage Event: An Update on the 1933
574 Long Beach, California, Earthquake, *The Seismic Record*. 3(2), 171–181, doi:
575 10.1785/0320230015.

576 Hough, S. E., and Graves, R. W. (2020) The 1933 Long Beach Earthquake (California, USA):
577 Ground Motions and Rupture Scenario, *Scientific Reports*, 10(1), 10017, 2020.
578 <https://doi.org/10.1038/s41598-020-66299>

579 Ishutov, S.(2013) Tectonic Characterization of the THUMS-Huntington Beach Fault,
580 Offshore Southern California, *SPE Western Regional/Pacific Section AAPG Conference*.

581 Lee, J., Tsai, V., Hirth, G., Chatterjee, A., Trugman, D.T. (2024) Fault-network geometry
582 influences earthquake frictional behaviour, *Nature*. DOI: 10.1038/s41586-024-07518-6

583 Lepper, R., B. Rhodes, M. Kirby, K. Scherer, J. Carlin, E. Hemphill-Haley, S. Avnaim-Katav,
584 G. MacDonald, S. Aranda, and A. Aranda, (2017), Evidence for coseismic subsidence
585 events in a southern California coastal saltmarsh, *Sci Rep* 7 44615.

586 <https://doi.org/10.1038/srep44615>

587 Ponti, D.J., Ehman, K.D., Edwards, B. D., Tinsley III, J.C., Hildenbrand, T., Hillhouse, J.W.,
588 Hanson, R.T., McDougall, K., Powell, C.L., II, Wan, E., Land, M., Mahan, S., Sarna-Wojcicki,
589 A.M. (2007) A 3- Dimensional Model of Water-Bearing Sequences in the Dominguez Gap
590 Region, Long Beach, California, *U.S. Geological Survey Open-File Report 2007-1013*, U.S.
591 *Department of the Interior U.S. Geological Survey*. <https://doi.org/10.3133/ofr20071013>

592 Yang, Yan and R. Clayton (2021), Shallow Seismicity in the Long Beach-Seal Beach, CA
593 Area, early publication, *Seismological Research Letters*,
594 <https://doi.org/10.1785/0220220358>.